(30) The occurrence of this band in the spectra of Ru(II) pyrazinium complexes provides a satisfactory explanation, within the framework of the trapped-valence model, of the weak shoulder at ~850 nm in the spectrum of the mixed valence

ion (see ref 4). It has been pointed out to us by a referee that owing to the large magnitude of spin-orbit coupling constants for Ru and Os (G. A. Crosby, K. W. Hipps, and W. H. Elkins, Jr., *J. Am. Chem. Soc.*, **96**, 629 (1974)), there is some doubt in our assignment of the weak, long wavelength transitions. Our assignment does explain why the weak transitions are observed in Ru(II) complexes only when the interaction of π and π^* orbitals is large and is supported by the fact that the change in δ is the same whether calculated for Ru(II) or Os(II). For these reasons we prefer to retain our interpretation though admitting that we may have to revise it when more insight into the electronic spectra of these species is gained.

(31) Similar behavior is observed in the protonation of

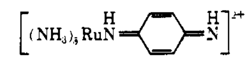

K. Rieder, U. Hauser, H. Siegenthaler, E. Schmidt, A. Ludi, to be submitted to *Inorg. Chem.*

(32) $\alpha_L = (\pi^*|H|\pi^*)$, $\alpha_M = (t_{2g}|H|t_{2g})$, $\beta = (\pi^*|H|t_{2g})$, and $\delta = \alpha_L - \alpha_M$.

Stereochemistry of Eight-Coordinate Mixed-Ligand Complexes of Zirconium. I. Characterization and the Crystal and Molecular Structure of Dinitratobis(acetylacetonato)zirconium(IV)[1]

Victor W. Day*[2a] and Robert C. Fay*[2b]

Contribution from the Departments of Chemistry, Cornell University, Ithaca, New York 14853, and University of Nebraska, Lincoln, Nebraska 68508.
Received July 27, 1974

Abstract: The crystal and molecular structure of dinitratobis(acetylacetonato)zirconium(IV), $Zr(acac)_2(NO_3)_2$, has been determined by single-crystal X-ray diffraction and has been refined (anisotropically on Zr, O, N, and C; isotropically on H) by least-squares methods to $R_1 = 0.036$ and $R_2 = 0.032$ using 3891 independent diffractometer-recorded reflections having $2\theta_{MoK\bar{\alpha}} < 63.7°$ and $I > 2\sigma(I)$. The compound crystallizes in the monoclinic space group $C2/c$ with eight molecules in a unit cell of dimensions: $a = 29.247$ (3), $b = 7.870$ (1), $c = 14.257$ (1) Å; $\beta = 93.824$ (8)° ($\rho_{obsd} = 1.669$, $\rho_{calcd} = 1.677$ g/cm^3). The crystal contains discrete eight-coordinate molecules in which bidentate acetylacetonate and bidentate nitrate ligands span the *m* edges of a (necessarily distorted) D_{2d}-$\bar{4}2m$ dodecahedron; each BAAB trapezoid contains one acetylacetonate and one nitrate ligand. Averaged Zr–O bond distances are: Zr–O(acac) 2.096 Å and Zr–O(nitrate) 2.295 Å. Within a particular chelate ring, the Zr–O bond lengths involving dodecahedral A sites exceed those involving B sites by 0.015–0.051 Å (5σ–17σ) and these differences appear to be propagated in the N–O and C–O bond lengths in the ligands, N–O_A being shorter than N–O_B by 0.012–0.019 Å (3σ–5σ) and C–O_A being shorter than C–O_B by 0.017–0.023 Å (4σ–6σ). The ligands are planar, and the acetylacetonate methyl groups adopt a conformation in which one methyl hydrogen atom and the -CH= hydrogen atom are eclipsed. The relative merits of the observed C_2-*mmmm* stereoisomer and other possible stereoisomers are discussed in terms of ligand bite, polyhedral edge lengths, and nonbonded contacts. In solution, $Zr(acac)_2(NO_3)_2$ is a monomeric nonelectrolyte which is stereochemically nonrigid on the NMR time scale at temperatures above −130°. Below −144°, stereochemical rearrangement is slow, and ^{1}H NMR spectra are consistent with the C_2-*mmmm* structure found in the solid state. Retention of coordination number eight in solution is indicated by the similarity of solid-state and solution-state infrared spectra.

In 1958 Brainina and coworkers[3] reported syntheses of the interesting, mixed-ligand zirconium complexes, $Zr(dik)_2(NO_3)_2$ and $Zr(dik)_3(NO_3)$, where dik represents the anion of acetylacetone or benzoylacetone. More recently some analogous hafnium complexes have been prepared.[4] These compounds have not yet been fully characterized, and nothing is known about their structures.

Structural points of interest include (1) the denticity of the nitrate ligands and the coordination number (CN) of the zirconium atom and (2) the geometry of the coordination polyhedron. For the dinitrato complexes, possible structures are $Zr(dik)_2(ONO_2)_2$ (CN 6), $Zr(dik)_2(O_2NO)(ONO_2)$ (CN 7), and $Zr(dik)_2(O_2NO)_2$ (CN 8), depending on the mode of nitrate attachment.[5] In addition to analogous structures for the mononitrato complexes, viz., $Zr(dik)_3(ONO_2)$ (CN 7) and $Zr(dik)_3(O_2NO)$ (CN 8), one must also consider an ionic structure, $[Zr(dik)_3]^+[NO_3]^-$, in which the zirconium atom exhibits CN 6.

Structures of the nitrato complexes are of interest in relation to previous structural work on halo(acetylacetonato)zirconium complexes and the tetrakisacetylacetonate. $Zr(acac)_3Cl$ is a pentagonal bipyramidal molecule (CN 7),[6] while $Zr(acac)_4$ adopts a square antiprismatic geometry (CN 8).[7] The detailed geometry of $Zr(acac)_2Cl_2$ is not yet known; however, NMR, infrared, Raman, and dipole moment studies point to a cis octahedral structure in solution.[8]

In this paper we report the characterization and the crystal and molecular structure of dinitratobis(acetylacetonato)zirconium(IV), $Zr(acac)_2(NO_3)_2$. A following paper will deal with $Zr(acac)_3(NO_3)$.

Experimental Section

Preparation and Physical Data. Dinitratobis(2,4-pentanedionato)zirconium(IV), $Zr(acac)_2(NO_3)_2$, was prepared in 63% yield according to the procedure of Brainina et al.[3] by reaction of acetylacetone with $ZrO(NO_3)_2 \cdot 2H_2O$ in benzene solution. Recrystallization from hot benzene-hexane (~40:60 v/v), under a dry nitrogen atmosphere, gave colorless crystals which were washed with dry hexane and dried in vacuo for 12 hr at room temperature: mp 149–151°, lit.[3] 146–148°; mol wt 392 (cryoscopic, 0.0327 *m* nitrobenzene solution), calcd 413; molar conductance 0.63 ohm^{-1} cm^2 mol^{-1} (1.00×10^{-3} *M* nitrobenzene solution, 25.0°); NMR (CH_2Cl_2 solution, 10.0 g/100 ml, 37°): −2.12 (CH_3) and −5.93 ppm (-CH=) relative to an internal reference of tetramethylsilane (1% by volume); ir (CH_2Cl_2 solution) ν_s(C⩦O) 1557 cm^{-1} and ν_{as}(C⩦O) 1353 cm^{-1}.

Crystallography. Single crystals of $Zr(acac)_2(NO_3)_2$, suitable for X-ray work, were grown from a dichloromethane–hexane mixture and were sealed under nitrogen in thin-walled glass capillaries for all subsequent X-ray studies. Weissenberg and precession photographs used to determine the probable space group and a preliminary set of lattice constants indicated monoclinic, $2/m$, symmetry. The systematically absent reflections were those required by space group Cc-C_s[4] (No. 9) or $C2/c$-C_{2h}[6] (No. 15). The choice of the centrosymmetric space group, $C2/c$, was fully supported by the negative results of sensitive tests for piezoelectricity made with a Geibe–Schiebe detector and by all stages of the subsequent structure determination. Use of the accurate lattice constants given below for a unit cell containing eight $Zr(acac)_2(NO_3)_2$ molecules gave a calculated density of 1.677 g/cm^3, in excellent agreement with the observed density of 1.669 g/cm^3 measured by flotation in a mixture of hexane, carbon tetrachloride, and 1,1,2,2-tetrabromoethane.

The simple atomic arrangement in the crystal was determined by the straightforward application of the heavy-atom technique using photographically recorded and three-dimensionally correlated diffraction data whose intensities were visually estimated by comparison with a "standard" intensity strip. Twenty-four interpenetrating layers of equiinclination Weissenberg intensity data, 9 along *b* and 15 along *c*, were recorded using multiple-film techniques with Zr-filtered Mo K$\bar{\alpha}$ radiation. The visually estimated intensities were reduced to relative squared amplitudes, $|F_o|^2$, by means of standard Lorentz and polarization factors. The 2356 independent data which resulted from the three-dimensional correlation of the relative $|F_o|^2$ values were used to calculate a Patterson synthesis, from which the Zr atom was located. A single difference Fourier synthesis at this point was sufficient to locate all remaining non-hydrogen atoms of the totally general-position asymmetric unit. Unit-weighted block-diagonal least-squares refinement employing anisotropic thermal parameters for all non-hydrogen atoms resulted in a conventional unweighted residual

$$R_1 = \Sigma \| F_o| - |F_c\| / \Sigma |F_o|$$

of 0.091. Bond lengths and angles calculated from the refined structural parameters at this point indicated CN 8 for the Zr atom with each bidendate ligand spanning an *m* edge of a (necessarily distorted) D_{2d} dodecahedron.[9] Although the Zr–O bonds to A-site oxygen atoms were systematically longer than those to B-site oxygen atoms within the same ligand (see Figure 1), the differences were not statistically significant since the estimated standard deviation in an individual Zr–O bond length averaged 0.010 Å. It was therefore decided to re-collect a set of diffractometer data in the hope that a more complete and accurate set of diffraction data might enable us to better characterize these and other subtle differences existing among the various bonds.

A nearly cube-shaped specimen, 0.50 mm on an edge, of $Zr(acac)_2(NO_3)_2$ was cut from a larger single crystal in a glove bag under nitrogen and sealed in a thin-walled glass capillary and then very carefully aligned optically on a computer-controlled four-circle Syntex P$\bar{1}$ autodiffractometer. A total of 15 high-angle ($2\theta_{MoK\bar{\alpha}}$ > 35°) reflections, chosen to give a good sampling of reciprocal space and diffractometer settings, were used to align the crystal and calculate angular settings for each reflection. A least-squares refinement of the diffraction geometry for these 15 reflections, recorded at the ambient laboratory temperature of 20 ± 1° with Nb-filtered Mo K$\bar{\alpha}$ radiation (λ 0.71069 Å), gave the lattice constants a = 29.247 ± 0.003 Å, b = 7.870 ± 0.001 Å, c = 14.257 ± 0.001 Å, and β = 93.824 ± 0.008°.

Intensity measurements utilized Nb-filtered Mo K$\bar{\alpha}$ radiation and the θ–2θ scanning technique with a 3° takeoff angle and a normal-focus X-ray tube. A scanning rate of 3°/min was employed for the scan between 2θ settings 1.0° above and below the calculated Kα doublet values ($\lambda_{K\alpha_1}$ 0.70926 Å and $\lambda_{K\alpha_2}$ 0.71354 Å) of each reflection. Background counts, each lasting for half the total scan time, were taken at both ends of the scan range. A total of 5650 reflections having $2\theta_{MoK\bar{\alpha}}$ < 63.7° (1.5 times the number of data in the limiting Cu K$\bar{\alpha}$ sphere) were measured in concentric shells of increasing 2θ containing approximately 1900 reflections each. Six standard reflections, monitored every 300 reflections, gave no indication of misalignment and/or deterioration of the crystal.

The linear absorption coefficient of the crystal[10] for Mo K$\bar{\alpha}$ radiation is 0.72 mm^{-1}, yielding a μR of 0.22 for a spherical crystal having the same volume as the cube-shaped specimen actually used. Since the absorption of X-rays by a spherical crystal having μR = 0.22 is virtually independent of scattering angle,[11] and deviations from this absorption occasioned by the use of the cube-shaped specimen are practically negligible except for a trivial fraction of the reflections, no absorption corrections were made and the intensities were reduced to relative squared amplitudes, $|F_o|^2$, by means of standard Lorentz and polarization corrections.

Of the 5650 reflections examined, 1759 were rejected as objectively unobserved by applying the rejection criterion, $I < 2.0\sigma(I)$, where $\sigma(I)$ is the standard deviation in the intensity computed from

$$\sigma^2(I) = (C_1 + k^2B)$$

C_1 being the total count from scanning, k the ratio of scanning time to total background time (in this case, k = 1), and B the total background count. The remaining 3891 observed intensities were used to locate the hydrogen atoms and refine the structure.

Unit-weighted anisotropic full-matrix least-squares refinement to convergence of the structural parameters for the 23 non-hydrogen atoms followed by a difference Fourier synthesis permitted the location of all 14 hydrogen atoms in the asymmetric unit. Further cycles of unit-weighted full-matrix least-squares minimization of the function $\Sigma w(|F_o| - K|F_c|)^2$ (where K is the scale factor), which employed isotropic thermal parameters for hydrogen atoms and anisotropic thermal parameters for all other atoms, led to R_1 = 0.036 and a conventional weighted residual

$$R_2 = \{\Sigma w(|F_o| - K|F_c|)^2/\Sigma w|F_o|^2\}^{1/2}$$

of 0.038 for 3891 reflections. These and all subsequent refinement cycles employed anomalous dispersion corrections for the Zr atom[12] and a least-squares refineable extinction correction of the form $1/(1 + gI_c)^{1/2}$ (where the extinction coefficient, g, refined to a final value of 3.24×10^{-7}). Empirical weights ($w = 1/\sigma^2$) were then calculated from

$$\sigma = \sum_0^3 a_n|F_o|^n = 1.82 - 0.154 \times 10^{-1}|F_o| + 0.440 \times 10^{-4}|F_o|^2 + 0.261 \times 10^{-6}|F_o|^3$$

the a_n being coefficients derived from the least-squares fitting of the curve

$$\| F_o| - K|F_c\| = \sum_0^3 a_n|F_o|^n$$

where the F_c values were calculated from the fully refined model using unit weighting. The final cycles of least-squares refinement utilized these weights to refine hydrogen atoms isotropically and all other atoms anisotropically together with the scale factor and extinction coefficient to give final values of 0.036 and 0.032 for R_1 and R_2, respectively, for 3891 independent reflections. During the final cycle of refinement, no parameter shifted by more than 0.40σ, with the average shift (including shifts for hydrogen atoms) being 0.03σ. The final parameters from least-squares cycles utilizing the empirical weights did not differ significantly from the final parameters from cycles utilizing unit weights. The atomic form factors compiled by Cromer and Mann[13] were used in all structure factor calculations.

The following programs were used on an IBM 360/65 computer for this work: MAGTAPE, SCALEUP, and SCTFT2, data reduction programs written by V. W. Day; FORDAP, Fourier and Patterson synthesis program, a modified version of A. Zalkin's original program; ORFLSE, full-matrix lease-squares structure refinement program, a highly modified version of Busing, Martin, and Levy's original ORFLS; ORFFE, bond lengths and angles with standard deviations by Busing, Martin, and Levy; ORTEP2, thermal ellipsoid

Table I. Atomic Fractional Coordinates in Crystalline $Zr(acac)_2(NO_3)_2$[a]

Atom[b]	10^4x	10^4y	10^4z
Zr	1248.9 (1)	1775.2 (3)	2794.7 (2)
O_{a1}	1581 (1)	4138 (2)	3103 (1)
O_{a2}	1901 (1)	991 (2)	3280 (1)
O_{b1}	1044 (1)	−626 (2)	3267 (1)
O_{b2}	977 (1)	2385 (2)	4054 (1)
O_{c1}	763 (1)	3885 (3)	2244 (2)
O_{c2}	574 (1)	1326 (3)	1943 (2)
O_{c3}	130 (1)	3384 (4)	1399 (2)
O_{d1}	1445 (1)	−128 (3)	1645 (1)
O_{d2}	1511 (1)	2520 (3)	1370 (2)
O_{d3}	1739 (1)	677 (4)	354 (1)
N_c	469 (1)	2903 (4)	1837 (2)
N_d	1574 (1)	1002 (4)	1086 (2)
C_{a1}	2049 (1)	6462 (4)	3558 (3)
C_{a2}	1974 (1)	4585 (3)	3434 (2)
C_{a3}	2322 (1)	3447 (4)	3667 (2)
C_{a4}	2275 (1)	1699 (4)	3590 (2)
C_{a5}	2662 (1)	539 (5)	3872 (3)
C_{b1}	702 (2)	−3023 (5)	3907 (4)
C_{b2}	802 (1)	−1157 (4)	2917 (2)
C_{b3}	651 (1)	−107 (4)	4612 (2)
C_{b4}	754 (1)	1588 (4)	4678 (2)
C_{b5}	623 (1)	2632 (5)	5492 (2)

[a] Figures in parentheses are estimated standard deviations in the last significant figure. [b] Each symbol for an atom of a ligand carries a literal subscript to identify the particular ligand (a, b, c, or d) and a numerical subscript to distinguish between atoms of the same element within that ligand. Atoms are labeled in agreement with Figure 2.

plotting program by C. K. Johnson; and MPLANE, least-squares mean plane calculation program from L. F. Dahl's group.

Results and Discussion

Structure in the Solid State. Final atomic coordinates and thermal parameters for crystalline $Zr(acac)_2(NO_3)_2$ are presented in Tables I–III.[14] A model seen in perspective of the contents of the asymmetric unit specified by the atomic coordinates of Tables I and III is illustrated in Figure 2; each non-hydrogen atom is represented by an ellipsoid having the shape, orientation, and relative size concomitant with the thermal parameters listed in Table II (hydrogen atoms are represented by small spheres not representative of their true thermal motion).

The crystal contains discrete eight-coordinate molecules in which bidentate acetylacetonate and bidentate nitrate ligands span the *m* edges (see Figure 1) of a (necessarily distorted) D_{2d}-$\bar{4}2m$ dodecahedron. Each BAAB trapezoid contains one acetylacetonate and one nitrate ligand; thus the approximate molecular point group symmetry is C_2-2, the quasi-twofold axis passing through the midpoints of the opposite *b* edges (Figure 1) which connect atoms O_{a2} and O_{b2} and atoms O_{c2} and O_{d2} (Figure 2). Note that the atom numbering system reflects the quasi-twofold symmetry; for example, oxygen atoms which occupy dodecahedral A sites of Figure 1 have the numerical subscript 1 in Figure 2 while those which occupy B sites have the numerical subscript 2. Bond distances, polyhedral edge lengths, and bond angles in the ZrO_8 coordination group are presented in Tables IV and V. A perspective view (adapted from a computer-drawn diagram) of the coordination polyhedron is shown in Figure 3. Average polyhedron-shape parameters are compared with theoretical values in Table VI. The packing of $Zr(acac)_2(NO_3)_2$ molecules in the crystal is depicted in Figure 4. There are no unusually short intermolecular contacts.

In terms of the geometric criteria discussed by Lippard and Russ,[15] the choice of coordination polyhedron for $Zr(acac)_2(NO_3)_2$ (D_{2d}-$\bar{4}2m$ dodecahedron or D_{4d}-$\bar{8}2m$ square antiprism) is unambiguous. The angle between the two intersecting trapezoidal best planes defined by atoms Zr, O_{a1}, O_{a2}, O_{c1}, and O_{c2} and by atoms Zr, O_{b1}, O_{b2}, O_{d1}, and O_{d2} (Table IX) is 90.7° vs. 90.0° for a perfect dodecahedron and 77.4° for a perfect antiprism. Values of d_T, the average displacement of ligand atoms from the trapezoidal best planes, are 0.04 and 0.05 Å, respectively (0.0 Å for a perfect dodecahedron), while values of d_S, the average displacement of ligand atoms from the best planes through the

Table II. Thermal Parameters in Crystalline $Zr(acac)_2(NO_3)_2$[a]

	Anisotropic Parameters, Å²						
Atom[b]	B_{11}	B_{22}	B_{33}	B_{12}	B_{13}	B_{23}	Equiv isotropic B,[c] Å²
Zr	3.04 (1)	2.59 (1)	3.39 (1)	−0.34 (1)	0.48 (1)	−0.24 (1)	2.95
O_{a1}	3.7 (1)	2.8 (1)	5.5 (1)	−0.3 (1)	0.7 (1)	−0.2 (1)	3.8
O_{a2}	3.6 (1)	3.0 (1)	4.2 (1)	−0.3 (1)	0.0 (1)	−0.2 (1)	3.5
O_{b1}	4.8 (1)	2.8 (1)	4.6 (1)	−0.7 (1)	1.7 (1)	−0.4 (1)	3.8
O_{b2}	4.7 (1)	3.1 (1)	3.7 (1)	0.1 (1)	0.8 (1)	−0.3 (1)	3.7
O_{c1}	4.3 (1)	3.9 (1)	5.8 (1)	0.0 (1)	−0.7 (1)	0.1 (1)	4.6
O_{c2}	4.1 (1)	4.3 (1)	6.0 (1)	−0.2 (1)	−0.5 (1)	−0.9 (1)	4.7
O_{c3}	4.5 (1)	7.9 (2)	6.7 (1)	0.9 (1)	−1.5 (1)	0.3 (1)	6.0
O_{d1}	4.9 (1)	4.0 (1)	3.9 (1)	−0.1 (1)	0.9 (1)	−0.4 (1)	4.2
O_{d2}	5.9 (1)	4.3 (1)	5.1 (1)	−0.6 (1)	1.7 (1)	0.2 (1)	4.9
O_{d3}	4.8 (1)	8.4 (2)	3.9 (1)	1.0 (1)	1.5 (1)	−0.2 (1)	5.1
N_c	3.7 (1)	5.4 (1)	4.1 (1)	0.2 (1)	0.4 (1)	−0.1 (1)	4.3
N_d	3.0 (1)	5.4 (1)	3.8 (1)	0.2 (1)	0.5 (1)	0.0 (1)	3.9
C_{a1}	5.2 (2)	2.9 (1)	7.2 (2)	−0.7 (1)	0.2 (1)	−1.0 (1)	4.6
C_{a2}	4.1 (1)	3.1 (1)	3.6 (1)	−0.7 (1)	0.7 (1)	−0.5 (1)	3.4
C_{a3}	3.6 (1)	3.8 (1)	5.3 (1)	−0.8 (1)	−0.3 (1)	−0.9 (1)	4.0
C_{a4}	3.6 (1)	3.6 (1)	3.0 (1)	−0.1 (1)	0.4 (1)	−0.2 (1)	3.4
C_{a5}	4.1 (1)	4.6 (2)	5.1 (2)	0.6 (1)	−0.5 (1)	−0.5 (1)	4.5
C_{b1}	7.2 (2)	3.3 (1)	9.1 (3)	−1.1 (1)	3.8 (2)	−0.1 (2)	5.4
C_{b2}	3.5 (1)	3.2 (1)	4.6 (1)	−0.2 (1)	0.7 (1)	0.3 (1)	3.7
C_{b3}	4.3 (1)	3.7 (1)	3.9 (1)	0.2 (1)	1.1 (1)	0.6 (1)	3.9
C_{b4}	3.9 (1)	4.0 (1)	3.4 (1)	0.9 (1)	0.3 (1)	−0.1 (1)	3.7
C_{b5}	7.0 (2)	4.9 (2)	4.1 (1)	1.3 (2)	1.4 (2)	−0.5 (1)	4.9

[a] Numbers in parentheses are estimated standard deviations in the last significant figure. Anisotropic temperature factors are of the form $\exp[-(\beta_{11}h^2 + \beta_{22}k^2 + \beta_{33}l^2 + 2\beta_{12}hk + 2\beta_{13}hl + 2\beta_{23}kl)]$; the B_{ij} in Å² are related to the dimensionless β_{ij} employed during refinement as $B_{ij} = 4\beta_{ij}/a_i^*a_j^*$. [b] Each symbol for an atom of a ligand carries a literal subscript to identify the particular ligand (a, b, c, or d) and a numerical subscript to distinguish between atoms of the same element within that ligand. Atoms are labeled in agreement with Figure 2. [c] Isotropic thermal parameter calculated from $B = 4\{V^2\det(\beta_{ij})\}^{1/3}$.

Table III. Refined Parameters for Hydrogen Atoms in Crystalline $Zr(acac)_2(NO_3)_2$[a]

Atom[b]	Fractional coordinates			Isotopic thermal parameter B, Å^2
	10^3x	10^3y	10^3z	
H_{a11}	188 (1)	706 (5)	313 (3)	3.8 (8)
H_{a12}	235 (1)	674 (5)	366 (3)	5.1 (9)
H_{a13}	191 (1)	675 (5)	410 (3)	4.1 (8)
H_{a3}	261 (1)	389 (4)	389 (2)	3.4 (7)
H_{a51}	273 (1)	−13 (5)	339 (3)	3.4 (8)
H_{a52}	259 (1)	−21 (5)	441 (3)	5.0 (9)
H_{a53}	295 (1)	111 (5)	406 (3)	4.6 (9)
H_{b11}	46 (2)	−318 (8)	338 (4)	9.7 (14)
H_{b12}	54 (2)	−332 (6)	440 (4)	7.2 (11)
H_{b13}	94 (2)	−376 (6)	375 (3)	6.0 (11)
H_{b3}	48 (1)	−60 (4)	507 (2)	2.2 (6)
H_{b51}	86 (1)	314 (5)	571 (2)	3.9 (8)
H_{b52}	45 (1)	204 (5)	595 (3)	5.9 (10)
H_{b53}	42 (1)	358 (5)	525 (3)	5.9 (9)

[a] Figures in parentheses are estimated standard deviations in the last significant figure. [b] Each symbol for a hydrogen atom carries the same (two) subscripts as the carbon atom to which it is bonded. In addition, methyl hydrogens carry a third subscript to distinguish between hydrogens on the same carbon atom. Atoms are labeled in agreement with Figure 2.

Table IV. Bond Distances in the Coordination Group of $Zr(acac)_2(NO_3)_2$[a]

Bond[b]	Length, Å	$(Zr-O_A)-(Zr-O_B)$, Å
$Zr-O_{a1}$	2.130 (2)	0.051 (3)
$Zr-O_{a2}$	2.079 (2)	
$Zr-O_{b1}$	2.106 (2)	0.038 (3)
$Zr-O_{b2}$	2.068 (2)	
$Zr-O_{c1}$	2.290 (2)	0.015 (3)
$Zr-O_{c2}$	2.275 (2)	
$Zr-O_{d1}$	2.321 (2)	0.027 (3)
$Zr-O_{d2}$	2.294 (2)	
Av values[c]		
Zr−O(acac)	2.096 (2, 22, 34)	
$Zr-O(NO_3^-)$	2.295 (2, 13, 26)	

[a] Figures in parentheses are estimated standard deviations in the last significant figure. [b] Oxygen atoms carry a literal subscript to identify the particular ligand (a, b, c, or d) and a numerical subscript to distinguish between atoms of the same ligand. Oxygen atoms occupying dodecahedral A sites of Figure 1 have the numerical subscript 1 while those occupying B sites have the numerical subscript 2. Atoms are labeled in agreement with Figure 2 and Tables I and II. [c] The numbers in parentheses following each averaged value are the root mean square estimated standard deviation for an individual datum and the mean and maximum deviation from the average value.

two "square faces" of the "antiprism", are 0.27 and 0.23 Å[16] (0.0 Å for a perfect antiprism).

Distortion of the ZrO_8 dodecahedron from full D_{2d}-$\bar{4}2m$ symmetry is necessitated by the chemical nonequivalence of the ligands and is most evident in the Zr-O bond distances and in the lengths of the m edges. The Zr-O(acac) bonds are ~0.20 Å shorter (and are presumably stronger and more covalent) than the $Zr-O(NO_3^-)$ bonds (cf. Table IV), and the m edges spanned by the acetylacetonate ligands are ~0.52 Å longer than those spanned by the nitrate ligands (cf. Table V and Figure 3). The length of an m edge corresponds to the "bite" of the ligand and is determined primarily by the ligand geometry and the number of atoms in the metal-chelate ring. Other polyhedral edges of the same class (a, b, or g) have rather similar lengths (cf. Table V). Mean plane calculations on the trapezoidal planes defined by the ligand oxygen atoms (i.e. Zr atom excluded; cf. Table IX) indicate that the inequality between the Zr-O(acac) and $Zr-O(NO_3^-)$ bonds is associated with small

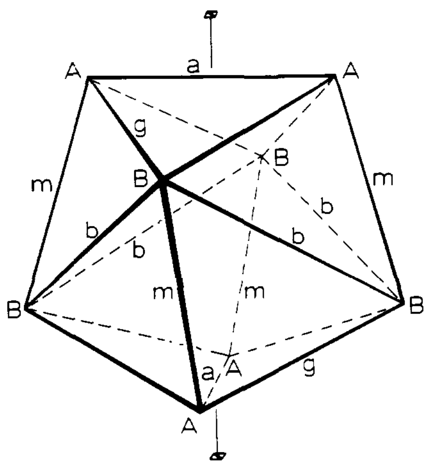

Figure 1. The D_{2d}-$\bar{4}2m$ dodecahedron, with vertices and edges labeled according to Hoard and Silverton.[9] Equivalent trapezoids, BAAB, lie in the mutually perpendicular mirror planes and interlock in agreement with $\bar{4}$. The ligand A sites and B sites are located, respectively, at the corners of two nonequivalent, interpenetrating D_{2d}-$\bar{4}2m$ tetrahedra, the A-site tetrahedron being elongated along the $\bar{4}$ axis and the B-site tetrahedron being compressed along the $\bar{4}$ axis. The 18 dodecahedral edges are distributed among four classes: a (2), b (4), m (4), and g (8). Each of the two mutually perpendicular twofold axes passes through the midpoints of a pair of opposite b edges.

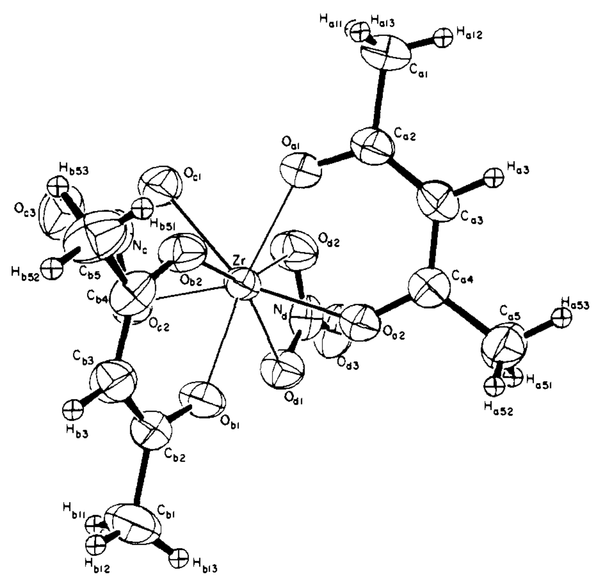

Figure 2. Model in perspective of the $Zr(acac)_2(NO_3)_2$ molecule. The quasi-twofold axis passes midway between atoms O_{a2} and O_{b2} and atoms O_{c2} and O_{d2}.

displacements of the Zr atom from these trapezoidal planes in the direction of the acetylacetonate ligands; thus the Zr atom is displaced 0.19 Å from the mean plane defined by atoms O_{a1}, O_{a2}, O_{c1}, and O_{c2} (displacement toward acac ligand b) and 0.09 Å from the mean plane defined by atoms O_{b1}, O_{b2}, O_{d1}, and O_{d2} (displacement toward acac ligand a). The averaged Zr-O(acac) bond length (2.096 Å) is shorter than the averaged Zr-O bond lengths in the eight-coordinate $Zr(acac)_4$ (2.198 Å),[7] seven-coordinate $Zr(acac)_3Cl$ (2.129 Å),[6] and pseudo-six-coordinate $(\pi-C_5H_5)Zr(acac)_2Cl$ (2.15 Å).[17] This suggests that $Zr(acac)_2(NO_3)_2$ could be regarded as a pseudo-octahedral, six-coordinate complex with each nitrate ligand being considered to occupy only one coordination site.[18] Alternatively, the Zr-O(acac) bonds may simply be shortened at the expense of the $Zr-O(NO_3^-)$ bonds since the averaged

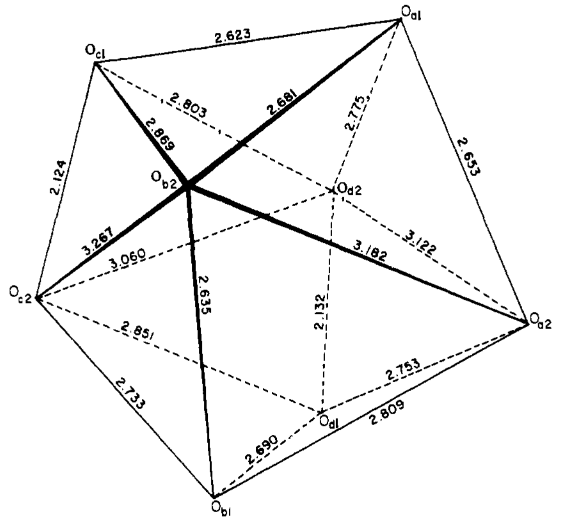

Figure 3. Perspective view (adapted from a computer-drawn diagram) of the dodecahedral coordination polyhedron as observed in the $Zr(acac)_2(NO_3)_2$ molecule. The four short edges of length 2.124, 2.132, 2.635, and 2.653 Å are the dodecahedral *m* edges spanned by the four bidentate ligands.

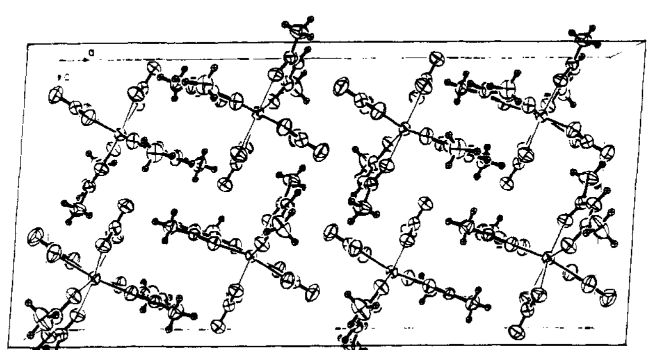

Figure 4. Model in perspective to illustrate the packing of $Zr(acac)_2(NO_3)_2$ molecules in the crystalline arrangement. The contents of one unit cell are viewed normal to the (010) plane.

length of all eight Zr-O bonds in the $Zr(acac)_2(NO_3)_2$ (2.195 Å) is nearly identical with the averaged Zr-O bond length in $Zr(acac)_4$.

It will be noted from Table IV that the Zr-O bonds directed toward the dodecahedral A sites (Figure 1), $Zr-O_A$, are significantly longer than the bonds directed toward the B sites, $Zr-O_B$. This is the case for all four ligands, the difference between $Zr-O_A$ and $Zr-O_B$ ranging from 0.015 Å (5σ) to 0.051 Å (17σ). Similar differences in the $M-L_A$ and $M-L_B$ bond distances have been observed for $Zr(C_2O_4)_4^{4-}$ (~0.06 Å)[19] and $Ti(S_2CNEt_2)_4$ (~0.08 Å),[20] which also have an *mmmm* dodecahedral structure. The ratio of the averaged bond distances, $Zr-O_A/Zr-O_B$, in $Zr(acac)_2(NO_3)_2$ is 1.015, compared with 1.00 for the hard sphere model and 1.03 for the D_{2d}-$\bar{4}2m$ dodecahedron which minimizes closed-shell ligand repulsions.[9] Relative lengthening of the $Zr-O_A$ bonds reduces $O_A \cdots O_A$ ligand repulsions along the *a* edges, the shortest of the polyhedral edges not spanned by a bidentate ligand (Table V). It is possible, as suggested by Colapietro et al. for $Ti(S_2CNEt_2)_4$,[20] that π bonding ($O_Bp\pi \rightarrow Zr\ d_{x^2-y^2}$) may also contribute to the difference between the $Zr-O_A$ and the $Zr-O_B$ bond lengths. In this connection it is interesting to note (Table IV) that the difference in bond lengths is greater for the Zr-O(acac) bonds than for the $Zr-O(NO_3^-)$ bonds.

Table V. Polyhedral Edge Lengths and Bond Angles Subtended at the Zr(IV) Atom in the Coordination Group of $Zr(acac)_2(NO_3)_2$[a]

Edge type[b]	Atoms[c]	Length, Å	Atoms[c]	Angle, deg
a	$O_{a_1}-O_{c_1}$	2.623 (3)	$O_{a_1}-Zr-O_{c_1}$	72.68 (8)
a	$O_{b_1}-O_{d_1}$	2.690 (3)	$O_{b_1}-Zr-O_{d_1}$	74.68 (7)
b	$O_{a_2}-O_{b_2}$	3.182 (3)	$O_{a_2}-Zr-O_{b_2}$	100.21 (8)
b	$O_{a_2}-O_{d_2}$	3.122 (3)	$O_{a_2}-Zr-O_{d_2}$	90.98 (8)
b	$O_{b_2}-O_{c_2}$	3.267 (3)	$O_{b_2}-Zr-O_{c_2}$	97.41 (8)
b	$O_{c_2}-O_{d_2}$	3.060 (3)	$O_{c_2}-Zr-O_{d_2}$	84.07 (8)
m	$O_{a_1}-O_{a_2}$[d]	2.653 (3)	$O_{a_1}-Zr-O_{a_2}$	78.14 (7)
m	$O_{b_1}-O_{b_2}$[d]	2.635 (3)	$O_{b_1}-Zr-O_{b_2}$	78.26 (7)
m	$O_{c_1}-O_{c_2}$[d]	2.124 (3)	$O_{c_1}-Zr-O_{c_2}$	55.46 (7)
m	$O_{d_1}-O_{d_2}$[d]	2.132 (3)	$O_{d_1}-Zr-O_{d_2}$	55.01 (8)
g	$O_{a_1}-O_{b_2}$	2.681 (3)	$O_{a_1}-Zr-O_{b_2}$	79.33 (7)
g	$O_{a_2}-O_{b_1}$	2.809 (3)	$O_{a_2}-Zr-O_{b_1}$	84.33 (7)
g	$O_{a_1}-O_{d_2}$	2.775 (3)	$O_{a_1}-Zr-O_{d_2}$	77.58 (8)
g	$O_{b_1}-O_{c_2}$	2.733 (3)	$O_{b_1}-Zr-O_{c_2}$	77.08 (8)
g	$O_{a_2}-O_{d_1}$	2.753 (3)	$O_{a_2}-Zr-O_{d_1}$	77.24 (7)
g	$O_{b_2}-O_{c_1}$	2.869 (3)	$O_{b_2}-Zr-O_{c_1}$	82.15 (8)
g	$O_{c_1}-O_{d_2}$	2.803 (3)	$O_{c_1}-Zr-O_{d_2}$	75.40 (8)
g	$O_{c_2}-O_{d_1}$	2.851 (3)	$O_{c_2}-Zr-O_{d_1}$	76.66 (7)
Av values[e]				
a	O···O	2.66 (0.3, 3, 3)	O-Zr-O	73.7 (0.8, 10, 10)
b	O···O	3.16 (0.3, 7, 11)	O-Zr-O	93.2 (0.8, 56, 91)
m	O···O	2.39 (0.3, 26, 27)	O-Zr-O	66.7 (0.7, 115, 117)
g	O···O	2.78 (0.3, 5, 10)	O-Zr-O	78.7 (0.8, 24, 56)

[a] Figures in parentheses are estimated standard deviations in the last significant figure. [b] Edge nomenclature is defined in Figure 1. [c] Oxygen atoms carry a literal subscript to identify the particular ligand (a, b, c, or d) and a numerical subscript to distinguish between atoms of the same ligand. Oxygen atoms occupying dodecahedral A sites of Figure 1 have the numerical subscript 1 while those occupying B sites have the numerical subscript 2. Atoms are labeled in agreement with Figure 2 and Tables I and II. [d] The "bite" of the ligand. [e] The numbers in parentheses following each averaged value are the root mean square estimated standard deviation for an individual datum and the mean and maximum deviation from the average value.

Table VI. Average Polyhedron-Shape Parameters[9] for $Zr(acac)_2(NO_3)_2$

Parameter[a]	$Zr(acac)_2(NO_3)_2$	MFP[b]	HSM[c]
a	1.21	1.17	1.20
b	1.44	1.49	1.50
m	1.09	1.17	1.20
g	1.27	1.24	1.20
θ_A, deg	36.8	35.2	36.9
θ_B, deg	75.7	73.5	69.5
$Zr-O_A/Zr-O_B$	1.015	1.03	1.00

[a] *a*, *b*, *m*, and *g* are averaged lengths of the dodecahedral edges (Figure 1) in units of the averaged Zr-O bond distance (2.195 Å). θ_A and θ_B are the averaged angles which the $Zr-O_A$ and $Zr-O_B$ bonds, respectively, make with the $\bar{4}$ axis (Figure 1). [b] Most favorable coordination polyhedron, calculated[9] to minimize the closed-shell ligand repulsive energy. [c] Hard sphere model.

Mixed-ligand chelates of the type $M(XX)_2(YY)_2$ which adopt dodecahedral stereochemistry with an *mmmm* wrapping pattern may exist as two geometric isomers: (1) a C_{2v} isomer in which the *m* edges of each BAAB trapezoid (Figure 1) are spanned by ligands of the same type; i.e., both XX ligands are on one trapezoid, and both YY ligands are on the other, or (2) a C_2 isomer in which the *m* edges of each trapezoid contain one XX ligand and one YY ligand. The latter stereoisomer is observed in crystalline $Zr(acac)_2(NO_3)_2$ and is expected to be the more stable isomer whenever there is an appreciable difference between the

Table VII. Bond Lengths (Å) and Bond Angles (deg) in the Acetylacetonate Ligands[a]

Bond[b]	Ligand a	Ligand b	Av[b]	Angle	Ligand a	Ligand b	Av[b]
$O_1 \cdots O_2$[c]	2.653 (3)	2.635 (3)	2.644 (3, 9, 9)	$Zr-O_1-C_2$	135.3 (2)	135.3 (2)	135.3 (2, 0, 0)
				$Zr-O_2-C_4$	136.9 (2)	136.2 (2)	136.6 (2, 4, 4)
O_1-C_2	1.263 (3)	1.275 (3)	1.269 (3, 6, 6)	$O_1-C_2-C_1$	116.1 (3)	115.6 (3)	115.9 (3, 3, 4)
O_2-C_4	1.280 (3)	1.298 (3)	1.289 (3, 9, 9)	$O_2-C_4-C_5$	116.3 (3)	115.7 (3)	
C_2-C_3	1.379 (4)	1.384 (4)	1.380 (4, 5, 10)	$O_1-C_2-C_3$	123.2 (2)	123.0 (2)	122.9 (3, 3, 5)
C_3-C_4	1.386 (4)	1.370 (4)		$O_2-C_4-C_3$	122.4 (3)	122.8 (3)	
C_1-C_2	1.503 (4)	1.498 (5)	1.496 (4, 5, 7)	$C_1-C_2-C_3$	120.7 (3)	121.3 (3)	121.2 (3, 2, 5)
C_4-C_5	1.489 (4)	1.493 (4)		$C_3-C_4-C_5$	121.2 (3)	121.5 (3)	
C_3-H_3	0.94 (3)	0.93 (3)	0.94 (3, 1, 1)	$C_2-C_3-C_4$	124.0 (3)	123.4 (3)	123.7 (3, 3, 3)
				$C_2-C_3-H_3$	118 (2)	118 (2)	118 (2, 0, 1)
				$C_4-C_3-H_3$	118 (2)	119 (2)	
C_1-H_{11}	0.90 (4)	0.99 (6)		$C_2-C_1-H_{11}$	112 (3)	105 (4)	
C_1-H_{12}	0.92 (4)	0.90 (5)		$C_2-C_1-H_{12}$	113 (3)	111 (3)	
C_1-H_{13}	0.92 (4)	0.94 (5)	0.94 (4, 4, 9)	$C_2-C_1-H_{13}$	106 (2)	118 (3)	111 (3, 3, 7)
C_5-H_{51}	0.89 (4)	0.85 (4)		$C_4-C_5-H_{51}$	110 (2)	107 (2)	
C_5-H_{52}	1.01 (4)	0.96 (4)		$C_4-C_5-H_{52}$	112 (2)	115 (3)	
C_5-H_{53}	0.97 (4)	0.99 (4)		$C_4-C_5-H_{53}$	115 (2)	109 (2)	
				$H_{11}-C_1-H_{12}$	118 (3)	100 (4)	
				$H_{11}-C_1-H_{13}$	101 (3)	103 (4)	
				$H_{12}-C_1-H_{13}$	107 (3)	117 (4)	108 (3, 5, 10)
				$H_{51}-C_5-H_{52}$	108 (3)	116 (3)	
				$H_{51}-C_5-H_{53}$	105 (3)	103 (3)	
				$H_{52}-C_5-H_{53}$	106 (3)	106 (3)	

[a] Numbers in parentheses are estimated standard deviations in the last significant figure. [b] The numbers in parentheses following each averaged value are the root mean square estimated standard deviation for an individual datum and the mean and the maximum deviation from the average value. [c] The bite of the ligand.

Table VIII. Distances (Å) and Angles (deg) in the Nitrate Ligands[a]

Distance	Ligand c	Ligand d	Av[b]	Angle	Ligand c	Ligand d	Av[b]
$N-O_1$	1.266 (3)	1.267 (3)	1.267 (3, 1, 1)	O_2-N-O_3	123.3 (3)	123.1 (3)	123.4 (3, 3, 5)
$N-O_2$	1.285 (3)	1.279 (3)	1.282 (3, 3, 3)	O_1-N-O_3	123.9 (3)	123.2 (3)	
$N-O_3$	1.198 (3)	1.206 (3)	1.202 (3, 4, 4)	O_1-N-O_2	112.8 (2)	113.7 (2)	113.3 (2, 5, 5)
$O_1 \cdots O_2$[c]	2.124 (3)	2.132 (3)	2.128 (3, 4, 4)				
$O_1 \cdots O_3$	2.175 (3)	2.176 (3)	2.176 (3, 1, 1)	$Zr-O_1-N$	95.8 (2)	95.1 (2)	95.7 (2, 3, 6)
$O_2 \cdots O_3$	2.185 (3)	2.185 (3)	2.185 (3, 0, 0)	$Zr-O_2-N$	96.0 (2)	96.0 (2)	

[a] Numbers in parentheses are estimated standard deviations in the last significant figure. [b] The numbers in parentheses following each averaged value are the root mean square estimated standard deviation for an individual datum and the mean and maximum deviation from the average value. [c] The bite of the ligand.

bites of XX and YY.[21] A C_{2v} structure for $Zr(acac)_2(NO_3)_2$ would require that nonbonded contacts along the *g* edges decrease from the observed values (Table V) of 2.68–2.87 Å (av 2.78 Å) to a value of ~2.67 Å.[22] It appears that the relatively large bite of the acetylacetonate ligand does not permit two acac ligands to be located on the same trapezoid of a ZrO_8 dodecahedron; this view is supported by the fact that $Zr(acac)_3(NO_3)$ shuns the *mmmm* wrapping pattern in favor of the previously unobserved dodecahedral *abmg* arrangement[23] and $Zr(acac)_4$ deserts the dodecahedron (almost entirely) in favor of a square antiprism.[7] Among the dodecahedral stereoisomers enumerated by Hoard and Silverton[9] are two (*aabb* and *mmgg*) which may allow optimum matching of ligand bites and polyhedral edge lengths for complexes of the type $M(XX)_2(YY)_2$. In the case of $Zr(acac)_2(NO_3)_2$, the *mmgg* isomer, with acac ligands on the *g* edges, is not obviously inferior to the observed *mmmm* isomer; however, the *aabb* isomer, with NO_3^- ligands on the *a* edges,[24] is disfavored because the bite of the acac ligand (generally 2.6–2.9 Å[25]) is too short to properly span the *b* edges (~3.16 Å).

Bond lengths and angles within the acetylacetonate and nitrate ligands are presented in Tables VII and VIII, respectively, and the results of mean plane calculations on the ligands are included in Table IX. It is noteworthy that the differences between the $Zr-O_A$ and $Zr-O_B$ bond lengths (Table IV) appear to be propagated in the C-O and N-O bond lengths in the ligands, $C-O_A$ being shorter than $C-O_B$ by 0.017–0.023 Å (4σ–6σ) and $N-O_A$ being shorter than $N-O_B$ by 0.012–0.019 Å (3σ–5σ). As expected, the shorter C-O and N-O bonds are adjacent to the longer Zr-O bonds, and vice versa, thus preserving the quasi-twofold symmetry. Ligand bond distances and angles are in good agreement with the values found in other acetylacetonate[25] and nitrate[18] structures. As is always the case in structures which contain "symmetrically" bidentate nitrate groups,[26] the terminal N-O bonds (1.202 Å) are shorter and the N-O bonds involving the coordinated oxygen atoms (1.267 and 1.282 Å) are longer than the N-O bonds in the nitrate ion (1.245 Å[18]); also the O-N-O bond angles involving the coordinated oxygen atoms (113.3°) are appreciably less than 120°. The NO_3^- ligands are almost exactly planar (Table IX), while the seven atoms of each C_5O_2 acetylacetonate skeleton exhibit only minor departures from planarity; displacements from the C_5O_2 mean planes are ≤0.06 Å (average displacement 0.022 Å). The Zr atom is slightly displaced from the mean plane of each ligand (Table IX), which implies that the chelate rings are slightly folded along the *m* edges (O···O) of the dodecahedron. The dihedral angles between the ligand planes and the planes defined by the appropriate O-Zr-O group are 0.9, 5.6, 1.7, and 4.5° for rings a, b, c, and d, respectively. The direction of the fold in all four rings is clockwise as viewed down the pseudo-$\bar{4}$ axis of Figure 2; i.e. the uncoordinated parts of ligand a are folded toward ligand b, ligand b is folded toward ligand c, etc.

Although hydrogen atoms have been located in several metal acetylacetonate structures,[27] no attention seems to

Table IX. Least-Squares Mean Planes of the Form $AX + BY + CZ = D^a$

Plane no.	Atoms	A	B	C	D
	Trapezoidal Planes				
1	Zr, O_{a1}, O_{a2}, O_{c1}, O_{c2}	0.4585	0.0584	−0.8868	−1.7500
2	Zr, O_{b1}, O_{b2}, O_{d1}, O_{d2}	−0.8931	0.0744	−0.4437	−4.6177
3	O_{a1}, O_{a2}, O_{c1}, O_{c2}	0.4566	0.0755	−0.8865	−1.6846
4	O_{b1}, O_{b2}, O_{d1}, O_{d2}	−0.8929	0.0666	−0.4452	−4.6124
	Ligand Planes				
5	O_{a1}, O_{a2}, C_{a1}, C_{a2}, C_{a3}, C_{a4}, C_{a5}	0.3696	0.0494	−0.9279	−2.3421
6	O_{b1}, O_{b2}, C_{b1}, C_{b2}, C_{b3}, C_{b4}, C_{b5}	−0.8233	0.1905	−0.5347	−4.7911
7	N_c, O_{c1}, O_{c2}, O_{c3}	0.5569	0.0317	−0.8300	−1.4291
8	N_d, O_{d1}, O_{d2}, O_{d3}	−0.8825	0.0047	−0.4702	−4.6928
	Atoms and Their Displacements from Planes, Å				
1	Zr, 0.141; O_{a1}, −0.010; O_{a2}, −0.064; O_{c1}, −0.023; O_{c2}, −0.045				
2	Zr, 0.067; O_{b1}, −0.069; O_{b2}, 0.009; O_{d1}, 0.063; O_{d2}, −0.070				
3	O_{a1}, 0.006; O_{a2}, −0.003; O_{c1}, −0.007; O_{c2}, 0.005; Zr, 0.188				
4	O_{b1}, −0.060; O_{b2}, 0.037; O_{d1}, 0.070; O_{d2}, −0.047; Zr, 0.089				
5	O_{a1}, −0.007; O_{a2}, 0.009; C_{a1}, 0.013; C_{a2}, −0.001; C_{a3}, −0.017; C_{a4}, −0.003; C_{a5}, 0.006; Zr, 0.026; H_{a11}, −0.408; H_{a12}, −0.192; H_{a13}, 0.884; H_{a3}, −0.049; H_{a51}, −0.687; H_{a52}, 0.848; H_{a53}, −0.074				
6	O_{b1}, 0.047; O_{b2}, −0.030; C_{b1}, 0.018; C_{b2}, −0.014; C_{b3}, −0.061; C_{b4}, −0.021; C_{b5}, 0.062; Zr, −0.143; H_{b11}, −0.887; H_{b12}, 0.011; H_{b13}, 0.581; H_{b3}, −0.077; H_{b51}, 0.717; H_{b52}, 0.052; H_{b53}, −0.720				
7	N_c, 0.000; O_{c1}, 0.000; O_{c2}, 0.000; O_{c3}, 0.000; Zr, −0.060				
8	N_d, 0.001; O_{d1}, 0.000; O_{d2}, 0.000; O_{d3}, 0.000; Zr, 0.159				

[a] X, Y, and Z are orthogonal coordinates measured in Å along a, b, and c^*, respectively, of the crystallographic coordinate system.

have been paid to the orientation of the methyl groups. In $Zr(acac)_2(NO_3)_2$ one hydrogen atom of each of the four crystallographically independent methyl groups lies in (or near) the plane (Table IX) of the appropriate C_5O_2 group, and this hydrogen atom is eclipsed with H_{a3} or H_{b3}, the hydrogen atom on the middle carbon atom (cf. Figures 2 and 4). This conformation is less favorable sterically than the staggered conformation accessible by a 60° rotation about the $C-CH_3$ bond; however, the contacts between H_{a3} or H_{b3} and the nearest neighbor methyl hydrogen atoms (2.35–2.43 Å) are not excessively short compared with the van der Waals diameter of 2.4 Å[28] for hydrogen.[29] These contacts may be attractive. The methyl groups adopt the same eclipsed conformation in $Pt(acac)_2I_2$.[27a] However, the staggered conformation is found in Co(salen)(acac),[27b] and both staggered and eclipsed conformations are observed in $Sc(acac)_3$.[27c] Thus, the optimum conformation is probably determined by the interplay of several competing factors, including both intra- and intermolecular van der Waals interactions.

Structure in Solution. $Zr(acac)_2(NO_3)_2$ is a monomeric nonelectrolyte in nitrobenzene, and infrared spectra of dichloromethane solutions indicate that all carbonyl groups are coordinated to the metal. Moreover, similarity of solid state and solution infrared spectra make it seem unlikely that there is a change in the mode of nitrate coordination, with a consequent change in coordination number, on going from the solid state to solution; a detailed infrared and Raman study is in progress.

Proton NMR spectra of dichloromethane solutions at ambient temperature and $CHClF_2$ solutions at temperatures as low as −130° indicate that $Zr(acac)_2(NO_3)_2$ is stereochemically nonrigid on the NMR time scale. At lower temperatures, however, the single, time-averaged methyl resonance splits into two lines of equal intensity (coalescence temperature, $T_c = -144°$).[30] The spectra at temperatures below T_c (two $-CH_3$ resonances and one $-CH=$ resonance) suggest that $Zr(acac)_2(NO_3)_2$ exists in solution as a single stereoisomer having twofold symmetry. While these spectra do not define a unique structure, they are fully consistent with the C_2-$mmmm$ dodecahedral structure found in the solid state.

Acknowledgment is made to the National Science Foundation (Grant GP-30691X, R.C.F.) and to the donors of the Petroleum Research Fund, administered by the American Chemical Society (V.W.D.), for support of this research. We are also grateful to the University of Nebraska for a generous allocation of computer time.

Supplementary Material Available. A listing of structure factor amplitudes will appear following these pages in the microfilm edition of this volume of the journal. Photocopies of the supplementary material from this paper only or microfiche (105 × 148 mm, 24× reduction, negatives) containing all of the supplementary material for the papers in this issue may be obtained from the Journals Department, American Chemical Society, 1155 16th St., N.W., Washington, D.C. 20036. Remit check or money order for $4.50 for photocopy or $2.50 for microfiche, referring to code number JACS-75-5136.

References and Notes

(1) Presented before the Division of Inorganic Chemistry, 167th National Meeting of the American Chemical Society, Los Angeles, Calif., April 1974.
(2) (a) University of Nebraska; (b) Cornell University.
(3) E. M. Brainina, R. Kh. Freidlina, and A. N. Nesmeyanov, *Bull. Acad. Sci. USSR, Div. Chem. Sci.*, 910 (1958).
(4) E. M. Brainina and E. L. Mortikova, *Bull. Acad. Sci. USSR, Div. Chem. Sci.*, 2418 (1967).
(5) Monodentate (ONO_2) and bidentate (O_2NO) nitrate attachment are distinguished here by the number of oxygen atoms which stand nearer the metal atom in the formula.
(6) R. B. Von Dreele, J. J. Stezowski, and R. C. Fay, *J. Am. Chem. Soc.*, **93**, 2887 (1971).
(7) J. V. Silverton and J. L. Hoard, *Inorg. Chem.*, **2**, 243 (1963).
(8) (a) T. J. Pinnavaia and R. C. Fay, *Inorg. Chem.*, **7**, 502 (1968); (b) R. C. Fay and T. J. Pinnavaia, *ibid.*, **7**, 508 (1968); (c) N. Serpone and R. C. Fay, *ibid.*, **8**, 2379 (1969).
(9) J. L. Hoard and J. V. Silverton, *Inorg. Chem.*, **2**, 235 (1963).
(10) "International Tables for X-Ray Crystallography", Vol. III, "Physical and Chemical Tables", The Kynoch Press, Birmingham, England, 1968, p 166.
(11) Reference 10, Vol. II, "Mathematical Tables", 1967, p 302.
(12) D. T. Cromer, *Acta Crystallogr., Sect. A*, **18**, 17 (1965).
(13) D. T. Cromer and J. B. Mann, *Acta Crystallogr., Sect. A*, **24**, 321 (1968).
(14) See paragraph at end of paper regarding supplementary material.
(15) S. J. Lippard and B. J. Russ, *Inorg. Chem.*, **7**, 1686 (1968).
(16) These values apply to the "square faces" defined by atoms O_{a1}, O_{a2}, O_{d1}, and O_{d2} and by atoms O_{b1}, O_{b2}, O_{c1}, and O_{c2}, respectively. Values of d_5 for the "square faces" defined by atoms O_{a1}, O_{a2}, O_{b1}, and O_{b2} and by atoms O_{c1}, O_{c2}, O_{d1}, and O_{d2} are 0.38 and 0.22 Å, respectively.
(17) J. J. Stezowski and H. A. Eick, *J. Am. Chem. Soc.*, **91**, 2890 (1969).
(18) C. C. Addison, N. Logan, S. C. Wallwork, and C. D. Garner, *Q. Rev., Chem. Soc.*, **25**, 289 (1971).
(19) G. L. Glen, J. V. Silverton, and J. L. Hoard, *Inorg. Chem.*, **2**, 250 (1963).
(20) M. Colapietro, A. Vaciago, D. C. Bradley, M. B. Hursthouse, and I. F. Rendall, *J. Chem. Soc., Dalton Trans.*, 1052 (1972).
(21) If the nitrate ligand is considered to occupy only one coordination site,[18] the C_{2v} isomer may be regarded as a pseudo-octahedral trans isomer, and the dodecahedral C_2 isomer as a pseudo-octahedral cis isomer. In this sense the stereochemistry of $Zr(acac)_2(NO_3)_2$ is related to that of $Zr(acac)_2Cl_2$, which exists as the cis isomer in solution.[8]
(22) In calculating this contact, observed distances (Tables IV and V) were assumed (Zr–O(acac) = 2.096 Å, Zr–O(NO_3^-) = 2.295 Å, m edge (acac) = 2.64 Å, m edge (NO_3^-) = 2.13 Å, a edge (acac–acac) = 2.66 Å) and the length of the a edge connecting the two NO_3^- ligands was allowed to vary so as to equalize the lengths of the eight g edges. If the a edge (NO_3^-–NO_3^-) is maintained at 2.66 Å, four of the g edges are 2.46 Å and the other four are 3.09 Å.
(23) E. G. Muller, V. W. Day, and R. C. Fay, *J. Am. Chem. Soc.*, in press.
(24) Cf. $TiCl_4(diars)_2$, which has diarsine ligands on the a edges: R. J. H. Clark, J. Lewis, R. S. Nyholm, P. Pauling, and G. B. Robertson, *Nature*

(London), 192, 222 (1961).
(25) E. C. Lingafelter and R. L. Braun, *J. Am. Chem. Soc.*, 88, 2951 (1966).
(26) The division between symmetrically bidentate and unsymmetrically bidentate nitrate groups is, of course, arbitrary. Addison et al.[18] consider a coordinated nitrate group to be symmetrically bidentate if the two M-O bonds differ by less than 0.2 Å, and unsymmetrically bidentate, if the two M-O bonds differ by 0.2-0.7 Å. Thus, the nitrate groups in $Zr(acac)_2(NO_3)_2$ would ordinarily be considered to be symmetrically bidentate, despite the small but real differences in the two Zr-O and N-O bond lengths.
(27) See, for example, (a) P. M. Cook, L. F. Dahl, D. Hopgood, and R. A. Jenkins, *J. Chem. Soc., Dalton Trans.*, 297 (1973); (b) M. Calligaris, G. Manzini, G. Nardin, and R. Randaccio, *Ibid.*, 543 (1972); (c) T. J. Anderson, M. A. Newman, and G. A. Melson, *Inorg. Chem.*, 12, 927 (1973).
(28) L. Pauling, "The Nature of the Chemical Bond", 3rd ed., Cornell University Press, Ithaca, N.Y., 1960, p 260.
(29) It is well known that C-H distances determined by X-ray techniques are usually short by ~0.15 Å. However, the nearly parallel orientation of the C-H bonds for the eclipsed acac hydrogen atoms will tend to minimize the effect of this systematic error on the "short" intramolecular H···H contacts.
(30) J. K. Howie and R. C. Fay, unpublished results.

Reactivity Patterns of Chromocene, Molybdenocene, and Tungstenocene Reaction Systems. I. Carbonyl Complex Formation as a Probe of Coordinative Unsaturation[1a]

Kit L. Tang Wong[1b] and Hans H. Brintzinger*[1c]

Contribution from the Department of Chemistry, The University of Michigan, Ann Arbor, Michigan 48104, and Fachbereich Chemie, Universität Konstanz, D 7750 Konstanz, West Germany. *Received November 5, 1974*

Abstract: Carbon monoxide is found to form a monocarbonyl complex with chromocene. Whereas $(C_5H_5)_2Mo(CO)$ and $(C_5H_5)_2W(CO)$ are thermally stable compounds, we find that the formation of $(C_5H_5)_2Cr(CO)$ is reversible; the associated enthalpy and entropy changes are $\Delta H_f° = -18.8 \pm 0.5$ kcal/mol and $\Delta S_f° = -60 \pm 2$ eu. The dicarbonyl complexes $(C_5H_5)(C_5H_7)M(CO)_2$ are stable for all three group 6 metals, M = Cr, Mo, and W. Tungstenocene, on the other hand, is unique in forming a stable dicarbonyl complex $(C_5H_5)_2W(CO)_2$ which exceeds an 18-valence-electron configuration. Factors contributing to the increasing accessibility of the metal center in the series $(C_5H_5)_2Cr$, $(C_5H_5)_2Mo$, $(C_5H_5)_2W$ to CO coordination are discussed and put in parallel to reactions of these species with other types of substrates.

Some time ago, we and others have reported on remarkable gradations in reactivity among the coordinatively unsaturated group 6 transition metal metallocenes.[2-4] Chromocene appears to be a fairly nonreactive particle, whereas both molybdenocene and tungstenocene, generated as intermediates from a number of reaction systems, will undergo a variety of basic addition and insertion steps of potential interest for homogeneous catalysis. Of the three metallocenes, however, only tungstenocene is capable of inserting into the C-H bond of aromatic hydrocarbons. In order to gain a more detailed understanding of factors contributing to this variation in reactivity, we have undertaken a systematic study of the reactions of carbon monoxide with this series of coordinatively unsaturated particles, as a particularly simple and efficient probe for coordinative unsaturation.

To date, monocarbonyl complexes have been described for molybdenocene and tungstenocene,[3,4] but not for chromocene. A stable dicarbonyl complex of composition $(C_5H_5)(C_5H_7)Cr(CO)_2$, on the other hand, has long been known to arise as one of the products when chromocene is exposed to both CO and H_2.[5] Preliminary reports on a related complex derived from molybdenocene have appeared in the literature recently.[6] We wish to report here a more systematic characterization of these known species, as well as observations on the occurrence of novel carbonyl complexes for both chromocene and tungstenocene.

Results and Discussion

1. Formation and Properties of $(C_5H_5)_2Cr(CO)$. When solutions of chromocene in petroleum ether or toluene are exposed to carbon monoxide, one observes a change in the visible spectrum. At CO pressures increasing from about 100 Torr to one atmosphere or more, one observes a diminution and final disappearance of the characteristic chromocene absorption at 454 nm. The reversibility of this reaction is established by the reappearance of this absorption band upon removal of the CO atmosphere. In a series of analogous experiments, we were unable to detect any interaction of chromocene with hydrogen gas, ethylene, 2-butyne, or diphenylacetylene.

Since complex formation is far from stoichiometric at room temperature, we have further characterized the complex formed from chromocene and carbon monoxide at lower temperatures. One finds that a petroleum ether solution of chromocene takes up CO at −78° under formation of a brownish precipitate which is stable against loss of CO in vacuo at this temperature. When warmed to room temperature, this complex loses 1 mmol of CO per millimole of chromocene; this establishes the 1:1 composition of the carbonyl complex formed. A determination of the equilibrium constant for the reaction $(C_5H_5)_2Cr$ (sol) + CO (gas) $\rightleftharpoons$ $(C_5H_5)_2Cr(CO)$ (sol) (sol = in toluene solution) is most conveniently performed by measuring the equilibrium pressure of CO (gas) over a partially carbonylated chromocene solution; measurements at different temperatures then yield the reaction enthalpy for this complex formation reaction. From the data presented in Table I we determine a standard enthalpy of complex formation of -18.8 ± 0.5 kcal/mol and an associated entropy change of -60 ± 2 eu.[7]

In the ^1H NMR spectrum of a toluene-d_8 solution of the carbonyl complex one sharp singlet is observed at τ 6.06 ppm, consistent with chemical shifts obtained with comparable, diamagnetic C_5H_5 complexes. Above 0° there is an increasing broadening of the singlet at τ 6.06, due to the re-